Journal of Architectural Research and Development, 2026, Volume 10, Issue 2
https://ojs.bbwpublisher.com/index.php/JARD
Online ISSN: 2208-3537
Print ISSN: 2208-3529

Analysis of Reflection Crack Propagation and Its Influencing Factors in Asphalt Overlay on Old Cement Concrete Pavement Based on Finite Element Method

Li Xu, Chunlin Li, Yuqing Hou

School of Civil Engineering, Chongqing Jiaotong University, Chongqing 400074, China

Abstract: Reflective cracking is one of the primary early-stage distresses in asphalt overlays on existing cement concrete pavements (white-to-black resurfacing structures). To delve into its mechanical evolution mechanism, this study established a three-dimensional thermal-mechanical coupled numerical model using the finite element software ABAQUS and quantitatively analyzed the variations in the stress intensity factor (SIF) during crack propagation using the J-integral method. The study systematically investigated the influence of material modulus, structural layer thickness, and external loads (traffic and temperature) on the SIF. Sensitivity analysis results reveal that environmental temperature drops and vehicle overloading are the core drivers of reflective crack propagation, with significantly higher sensitivity than structural material properties. Increasing the thickness of the asphalt overlay generates a notable "bridging anti-cracking" effect, representing the most effective structural means to inhibit crack propagation. The research findings provide a theoretical basis for anti-cracking design and lifespan prediction in the rehabilitation of existing pavements.

Keywords: Asphalt overlay; Reflective cracking; Stress intensity factor; Thermal-mechanical coupled model; Sensitivity analysis

Online publication: Apr 5, 2026

1. Introduction

As China's highway construction focuses shifts towards maintenance and rehabilitation, white-to-black resurfacing projects have been widely adopted [1]. However, the joints or cracks in existing cement concrete panels represent inherent weak points in the structure. Under the combined effects of panel expansion and contraction caused by environmental temperature gradients and repeated traffic loads, high stress concentrations occur at the joints, easily inducing reflective cracks that propagate from the bottom up in the asphalt overlay [2]. Once reflective cracks penetrate the surface layer, surface water infiltrates, weakening the stiffness of the pavement base and accelerating structural failure. The Paris formula, as the most classical empirical model describing the stable propagation stage of fatigue cracks, provides a theoretical framework for quantitatively evaluating reflective cracks [3].

Current academic frontiers are shifting from single-field mechanical simulations to the deep integration of multi-field coupling and the application of new materials. Since 2024, research has indicated that the nonlinear interaction between the environmental temperature field and dynamic traffic loads is the root cause of extreme stress concentrations at the bottom of the overlay [4]. Simultaneously, the potential of new composite aggregates (such as partially replacing natural aggregates with industrial waste steel slag) to enhance the anti-cracking performance of overlays has garnered widespread attention [5]. The latest fracture mechanics evaluation models have begun incorporating stochastic damage theory and machine learning algorithms, aiming to more realistically simulate the crack propagation paths of pavements under complex service environments through multi-dimensional parameter simulations [6]. However, accurately identifying the weight contributions of material properties and geometric structural parameters to crack propagation remains a core challenge in anti-cracking design. Therefore, establishing a high-precision three-dimensional finite element thermal-mechanical coupled model and quantitatively evaluating the sensitivity of key parameters are of extremely significant practical importance for optimizing overlay structural schemes and enhancing engineering service life.

2. Finite element numerical simulation and computational methods

2.1. Computational theory of stress intensity factor (SIF)

The stress intensity factor (SIF, commonly denoted by the symbol K) is a core parameter that characterizes the stress field at the crack tip and is used to evaluate the risk of material fracture under specific loads. In the analysis of reflective cracking in asphalt overlays, the primary focus is on the equivalent stress intensity factors of Mode I (opening mode) and Mode II (shearing mode) induced by the coupled effects of load and temperature. To accurately handle the nonlinear and large deformation behaviors that asphalt mixtures may exhibit, this study employs the J-integral method from fracture mechanics to calculate the SIF [7]. The J-integral is path-independent, and its mathematical expression is as follows:

$$J = \int_{\Gamma} \left(W \mathrm{dy} - T_{\mathrm{i}} \frac{\partial \mathrm{u_i}}{\partial \mathrm{x_i}} \mathrm{ds} \right) \tag{1}$$

In the formula, Γ represents the strain energy density per unit volume; ui denotes the displacement components; σij signifies the stress components on the closed path boundary; and Γ is an arbitrary integration path encircling the crack tip.

Within the framework of linear elastic fracture mechanics (LEFM), the calculated energy release rate can be directly converted into the stress intensity factor:

$$J = \frac{K^2}{E} \tag{2}$$

In the formula, E represents the elastic modulus of the material. Through verification and analysis, the values calculated by this numerical method highly coincide with the theoretical analytical values in the classic “Stress Intensity Factor Handbook”, with a relative error of less than 0.01%, demonstrating the accuracy of the model [8].

2.2. Establishment of a three-dimensional thermal-mechanical coupled finite element model

Based on the ABAQUS finite element simulation platform, a three-dimensional thermal-mechanical coupled analysis model was constructed for the pavement structure consisting of an old cement concrete layer with an asphalt overlay. The model underwent a series of reasonable simplifications: it was assumed that each structural

layer was a continuous, homogeneous, and linearly elastic material, and that the interfaces between layers were fully bonded without relative slippage.

The reference structure of the model was composed of two old cement concrete slabs, each measuring 5 m × 4.5 m × 0.22 m, with an initial joint defect of 10 mm width reserved between them. A complete layer of asphalt overlay, measuring 10.01 m × 4.5 m × 0.10 m, was fully covering the slabs. See **Figure 1**.

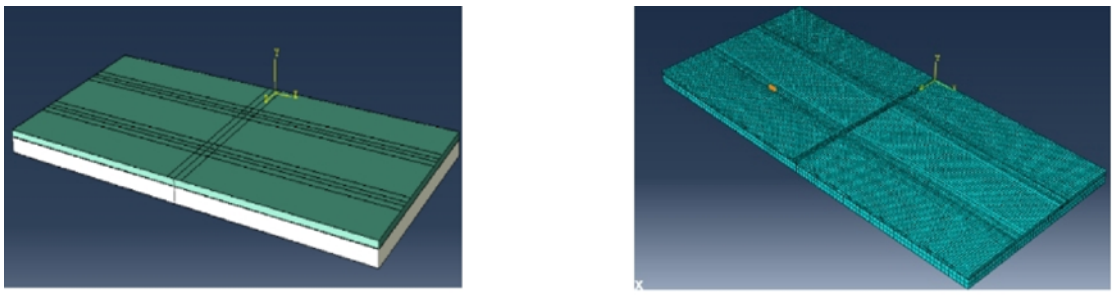

(a) (b)

Figure 1. Schematic diagram of the finite element model and mesh division for the three-dimensional pavement structure.

As shown in **Figure 1**, to ensure the accuracy of fracture mechanics parameter (stress intensity factor) calculations while also considering computational efficiency, this model employs coarser hexahedral meshes in areas far from the joints. In contrast, significant local mesh refinement is applied in regions near the joints and crack tips where crack propagation may occur (the densely meshed areas in the figure). This transitional mesh division approach not only accurately captures the high stress gradients at the crack tips but also effectively controls the overall number of degrees of freedom [9].

The relevant key mechanical and thermodynamic parameters of the materials are presented in **Table 1** and **Table 2**.

Table 1. Mechanical parameters of pavement structural layers

Structural layer	Thickness/cm	Modulus/MPa	Poisson's ratio
Asphalt layer	10	10000	0.3
Cement concrete layer	20–32	15000–30000	0.15

Table 2. Thermodynamic parameters of pavement structure layers

Structural layer	Density (kg/m^3)	Thermal conductivity coefficient (W/(m·K))	Coefficient of linear expansion(× 10 $^{-6}$/℃)	Specific heat capacity (J/(kg·K))
Asphalt layer	2400	1.2		1200
Cement concrete layer	2500	1.5		900

2.3. Load and temperature field settings

The structural calculations employ a "direct coupling" method for thermal-mechanical coupling. The traffic load is selected as a standard single-axle dual-wheel load (with an axle weight of 100 kN and a tire contact pressure of 0.7 MPa). Based on the principle of total stress equivalence, the dual-circle load is converted into an equivalent rectangular load, with a single wheel contact area measuring approximately 18.4 cm × 19.2 cm [10]. To obtain the most unfavorable working condition and stimulate the shear action at the crack tip, a biased load pattern is adopted, with the load placed on the edge of one side of the joint. See **Figure 2**.

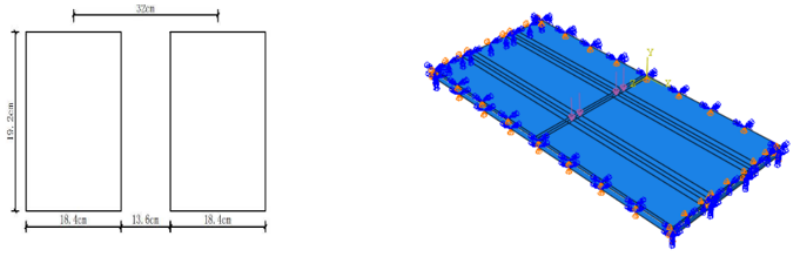

(a) Schematic diagram of rectangular load arrangement (b) Schematic diagram of wheel load arrangement

Figure 2. Schematic diagram of the biased load arrangement of a standard dual-wheel load at the joint.

Figure 2 illustrates the arrangement method for the most unfavorable load condition. This biased load pattern results in significant vertical relative displacement differences between the concrete slabs on both sides of the joint, thereby inducing intense shear-type (Mode II) stress concentration phenomena at the crack tip.

Regarding temperature loads, the model sets the initial temperature at 5 ℃, with a temperature gradient of 0.8 ℃/cm along the depth direction. The study selects a temperature range from 10 ℃ to 30 ℃ to simulate typical diurnal or seasonal temperature drops from mild to extremely cold regions.

3. Analysis of influencing factors and sensitivity on reflection crack propagation

3.1. Influence mechanism of material mechanical properties

Changes in the modulus of structural layers have a distinct primary and secondary regulatory effect on the stress field. An increase in the elastic modulus (Ec) of the old cement concrete base directly elevates the stress intensity level at the crack tip. As Ec increases from 15,000 MPa to 35,000 MPa, the opening-mode, shear-mode, and effective stress intensity factors all exhibit a monotonically increasing trend with increasing crack depth. See **Figure 3**.

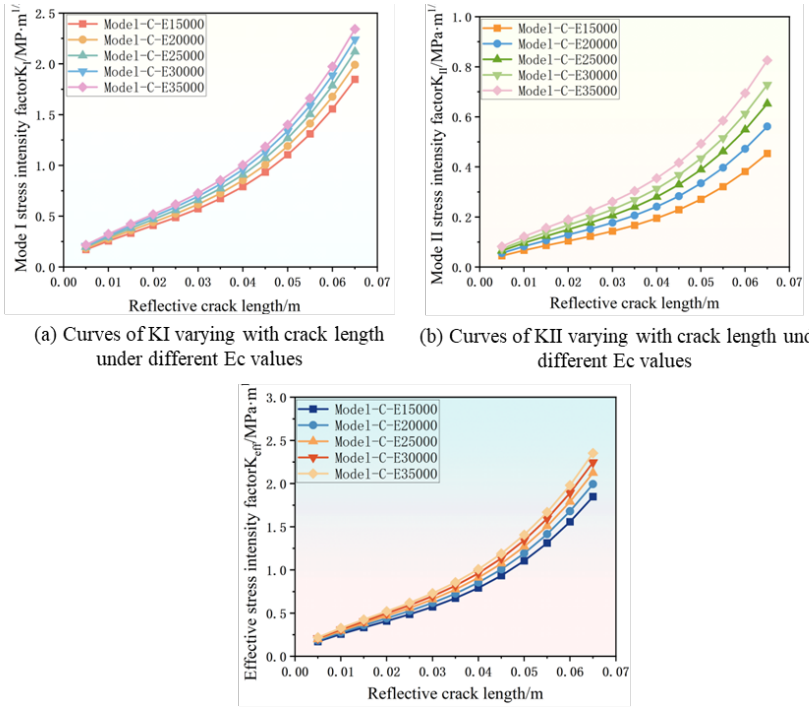

(a) Curves of KI varying with crack length under different Ec values

(b) Curves of KII varying with crack length under different Ec values

(c) Curves of Keff varying with crack length under different Ec values

Figure 3. The curves of stress intensity factors (SIFs) varying with crack length under different moduli (Ec) of the old concrete layer.

Based on **Figure 3**, during the initial stage of crack propagation (a < 0.04 m), the differences in SIFs under various moduli are minimal. When the crack penetrates into the middle to late stages of the surface layer (a > 0.04 m), the slope of the curves for the high-modulus group increases significantly. An excessively rigid base layer weakens the overall flexibility and coordination capacity of the structure, preventing the energy generated by traffic loads from being buffered through base layer bending. Consequently, this energy is forced to concentrate in a very small area at the crack tip, accelerating the risk of unstable propagation in the later stages [11].

On the other hand, an increase in the modulus (Ea) of the asphalt overlay also leads to a slight rise in stress intensity at the crack tip, but its magnitude of influence is significantly weaker than that of the concrete modulus. When the design modulus of the asphalt mixture is increased from 6000 MPa to 14000 MPa, the difference between the maximum and minimum SIF values fluctuates by only around 5% to 15%. See **Figure 4**.

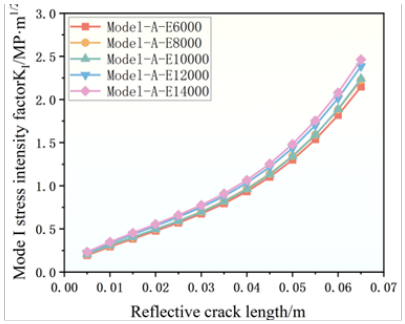

(a) Curves of KI varying with crack length under different Ea values

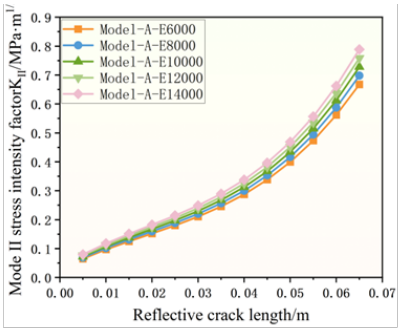

(b) Curves of KII varying with crack length under different Ea values

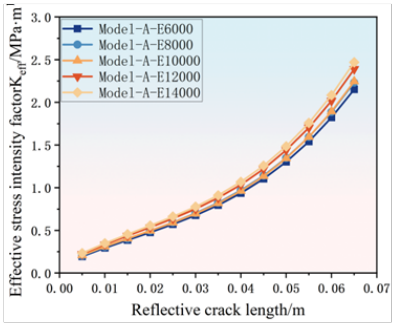

(c) Curves of Keff varying with crack length under different Ea values

Figure 4. The curves of stress intensity factors (SIFs) varying with crack length under different moduli (Ea) of the asphalt layer.

Figure 4 reveals that when the modulus of the asphalt layer increases from 6000 MPa to 14000 MPa, the SIF curves for all conditions exhibit a dense clustering characteristic. Even with a more than doubling of the modulus, the peak fluctuation range of SIFs remains strictly limited between 5% and 15%. As a viscoelastic flexible system, the asphalt surface layer, despite its slightly increased brittleness tendency at the microscale due to moderate stiffness enhancement, fails to alter the macroscopic stress distribution pattern dominated by the high-stiffness concrete slab system beneath [12].

3.2. The double-edged sword effect of structural parameters

In the design of structural layer thickness, adjustments to the base and surface layers often exhibit significant mechanical differences. Blindly increasing the thickness (hc) of the old concrete layer is detrimental to crack prevention, as the exacerbated mismatch in stiffness interfaces between the upper and lower layers promotes stress concentration at the crack tip. See **Figure 5**.

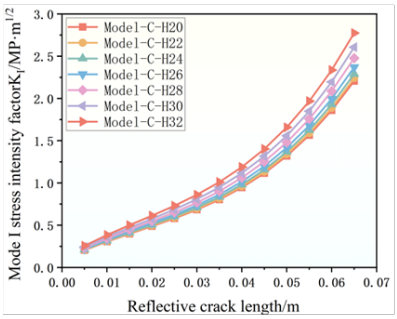

(a) Curves of KI varying with crack length under different hc values

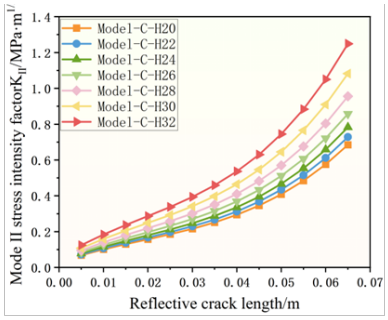

(b) Curves of KII varying with crack length under different hc values

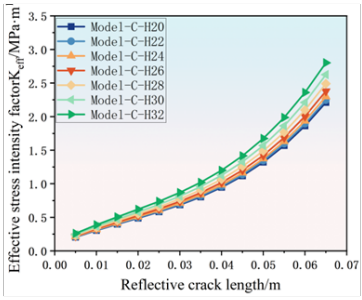

(c) Curves of Keff varying with crack length under different hc values

Figure 5. The curves of stress intensity factors (SIFs) varying with crack length under different thicknesses (hc) of the concrete layer.

The calculation results indicate that when hc increases from 20 cm to 32 cm, the overall stiffness of the foundation significantly rises, leading to a stiffness mismatch between the upper and lower interfaces. Under traffic loading, this mismatch causes stress to highly concentrate at the weak crack tip, triggering an abnormal increase in the stress intensity factor [13].

Increasing the thickness (ha) of the asphalt overlay serves as the most direct and effective structural measure to inhibit crack propagation. See **Figure 6**.

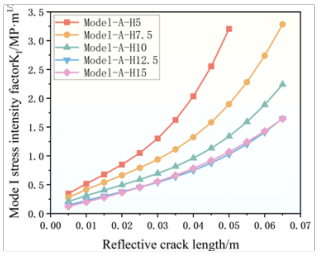

(a) Curves of KI varying with crack length under different ha valuesunder different hc values

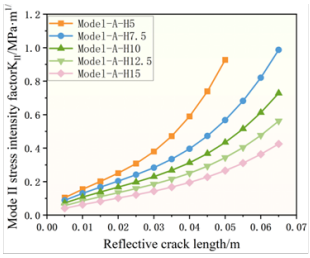

(b) Curves of KII varying with crack length under different ha values

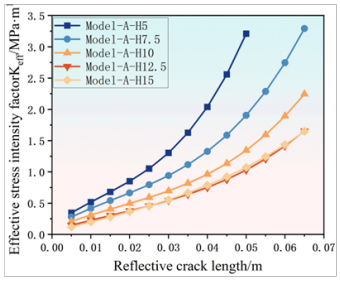

(c) Curves of Keff varying with crack length under different ha values

Figure 6. Curve depicting the impact of asphalt overlay thickness on SIF.

Figure 6 visually illustrates the "bridging crack prevention" effect brought about by an increase in the thickness of the asphalt surface layer [14]. As ha increases from 5 cm to 15 cm, the driving force rapidly disperses within the surface layer and exhibits a nonlinear decline. Data indicates that a thickness of around 10 cm can significantly alleviate abrupt changes in stiffness at the underlying layer, achieving the optimal crack prevention benefit ratio, while the marginal benefits of excessive thickening will gradually diminish.

3.3. Driving effects of external traffic and environmental loads

Vehicle overloading directly exacerbates incompatible deformations in the pavement structure at joints, inducing high-amplitude distortions in the stress field at crack tips. As external axle loads escalate from 1.0 times the standard axle load to 2.0 times the heavy-load condition, both Mode I (opening mode) and Mode II (shearing mode) stress intensity factors demonstrate significant stepwise amplification.

Figure 7 visually presents the evolutionary trajectories of SIFs under various overloading levels. In terms of overall magnitude, due to the direct downward bending and tension caused by the load, the Mode I stress intensity factor consistently remains higher than that of Mode II. During the critical stage where the crack steadily extends towards the surface layer and is on the verge of breakthrough, the relative increases in Mode I and Mode II stress intensity factors surge to 76.52% and 107.53%, respectively. The asymmetric placement of wheel loads towards the direction of the joint forces the rigid panels on both sides of the joint to undergo significant vertical relative displacement differences. This step-like local shear deformation is fully absorbed by the asphalt surface layer, causing the shear stress concentration effect at the crack tip to deteriorate superlinearly with load multiplication, serving as a direct mechanical driving force for premature fatigue shear failure of the pavement structure under heavy traffic conditions.

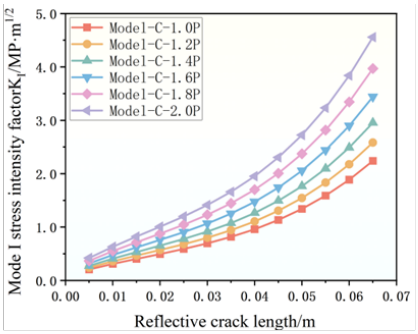

(a) Curve of KI variation with crack length under different overloading conditions

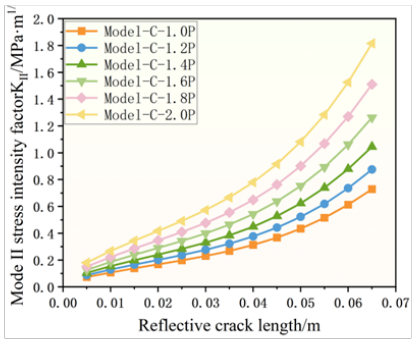

(b) Curve of KII variation with crack length under different overloading conditions

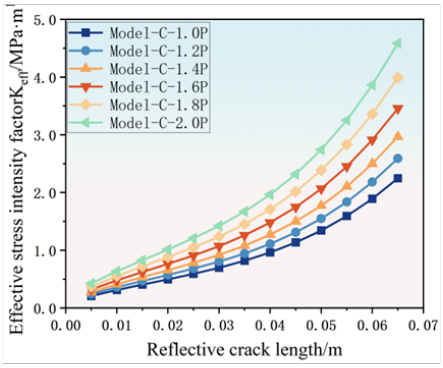

(c) Curve of Keff variation with crack length under different overloading conditions

Figure 7. Curves of SIF variation with crack length under different overload conditions.

Extreme cooling environments induce severe overall thermal contraction in asphalt overlays through thermo-mechanical coupling mechanisms. During cooling-induced shrinkage, the continuously paved large-area asphalt surface layer is subjected to strong frictional forces and displacement constraints from the underlying old cement concrete base with extremely high stiffness. The sharp drop in temperature gradient transforms into a substantial tensile stress reserve within the structure, exerting a powerful tearing effect on the Mode I (opening-mode) crack tips located at weak joints [15].

As shown in **Figure 8**, a 10 ℃ temperature drop causes a sharp increase of approximately 100.23% in the opening-mode SIF. When exposed to an extreme cold wave of 30 ℃, material embrittlement combined with high shrinkage tensile stresses drives the increase to an astonishing 469.08%. At this point, the crack tip energy release rate exceeds the material's toughness threshold, leading to unstable crack propagation and full-thickness penetration.

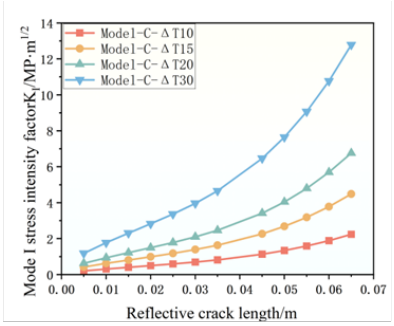

(a) Curve of Mode I stress intensity factor (KI) variation with crack length under different temperature drop ranges

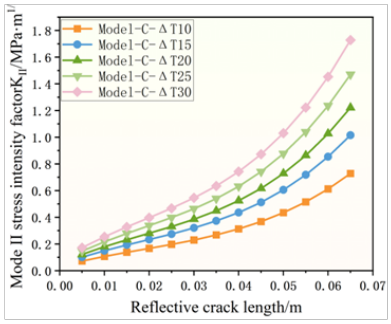

(b) Curve of Mode II stress intensity factor (KII) variation with crack length under different temperature drop ranges

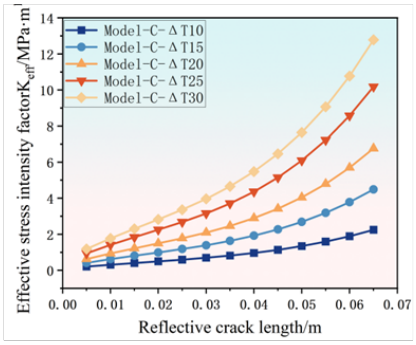

(c) Curve of effective stress intensity factor (Keff) variation with crack length under different temperature drop ranges

Figure 8. The curve of SIF variation with crack length during cooling.

There were essential differences in the mechanical dimensions between the driving mechanisms of external environment and traffic load on reflective cracking. The quantitative comparison between **Figure 9** and **Figure 10** profoundly reveals the similarities and differences in the damage characteristics of these two external incentives.

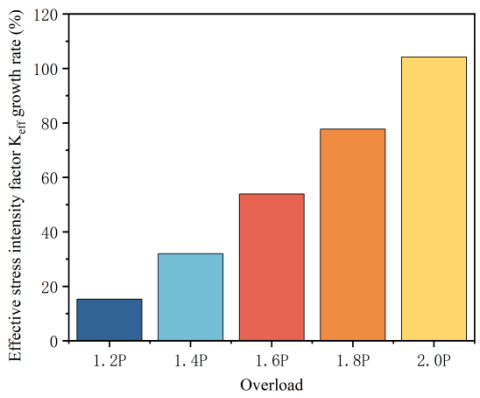

Figure 9. Growth rate of Keff under overload.

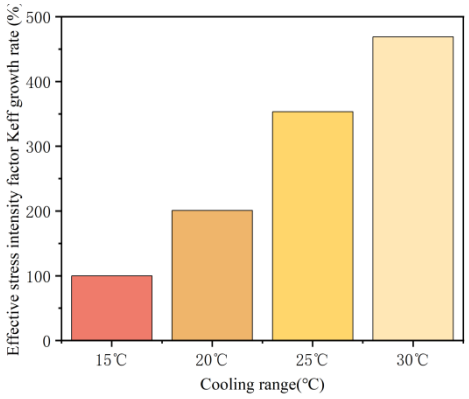

Figure 10. Growth rate under the influence of temperature drop magnitude.

By synthesizing the data evolution patterns from **Figure 7** to **Figure 10**, it can be observed that the growth rate of the stress intensity factor driven by traffic overload exhibits a relatively gentle and predictable linear evolution trend, with its damage energy primarily accumulating proportionally with the axle load tonnage. In contrast, the amplification effect of thermal contraction stress induced by extreme temperature drops on the driving force at the crack tip demonstrates a highly destructive exponential surge. In regions characterized by cold temperatures and significant daily temperature variations, the pure opening-mode (Mode I) fracture triggered by temperature gradients completely overwhelms the shear damage caused by traffic loads, becoming the absolute dominant factor leading to the rapid propagation of reflective cracks from the bottom to the top of the pavement surface. For pavement anti-cracking designs facing severe cold climatic conditions, it is essential to abandon the singular concept of resistance to load-induced fatigue and instead endow structural materials with higher deformation allowances and anti-cracking safety factors to counteract the extreme cold-induced thermal contraction stresses.

3.4. Comprehensive sensitivity assessment of various factors

To quantitatively determine the primary and secondary impacts of various factors on reflective cracking, this study employed sensitivity tornado diagrams to conduct dimensionless and normalized comparisons of multiple variables [16]. The span of the bands in the diagram represents the comprehensive influence weight of each parameter on the crack driving force under extreme fluctuations. See **Figure 11**.

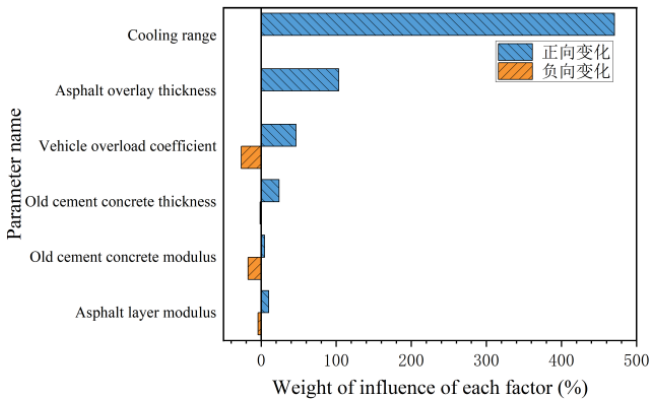

Figure 11. Tornado diagram of parameter sensitivity for driving forces in the propagation of reflective cracks

As shown in **Figure 11**, the calculated data intuitively reveals the mechanical sensitivity rankings of various parameters. At the top of the chart, "temperature drop range" dominates with an upper limit impact of 470.66%, followed by "vehicle overload", which exceeds 103% in influence. Among structural layer parameters, fluctuations in "asphalt surface layer thickness" provide a stress intensity regulation range of up to 73.16% (-26.61% to 46.55%), making it the only structural means to effectively counteract external loads. At the bottom, the combined impacts of "old cement concrete slab thickness", "concrete modulus", and "asphalt layer modulus" are only 25.36%, 22.12%, and 14.11%, respectively.

The sensitivity ranking of driving forces for reflective crack propagation is precisely defined as follows: temperature drop > vehicle overload > thickness of asphalt overlay > thickness of old cement concrete slab > concrete modulus > asphalt layer modulus. Core resources for anti-cracking design should be allocated to limiting heavy traffic, implementing tolerance designs for local extreme climates, and moderately thickening the asphalt overlay. Simply increasing material modulus cannot fundamentally impede the evolution of reflective cracks.

4. Conclusions and engineering design recommendations

This study reveals the evolution patterns of reflective cracks through three-dimensional thermo-mechanical coupled finite element simulations. The results indicate that environmental cooling and vehicle overload are the primary drivers of crack propagation, with temperature-induced opening-mode stress intensity factors growing exponentially, serving as the core failure mechanism for overlays in cold regions. Structurally, thickening the asphalt layer effectively prevents cracking through "bridging effects", while blindly thickening the concrete slab leads to adverse stress concentration due to stiffness mismatch. The sensitivity ranking is as follows: temperature drop > axle load > overlay thickness > old pavement slab thickness > material modulus.

Based on these findings, it is recommended to prioritize optimizing thickness configurations in design, with an asphalt overlay thickness of over 10 cm to alleviate stress mutations at the base layer. Material selection should abandon high-modulus approaches in favor of low-modulus, high-flexibility systems incorporating composite aggregates like steel slag [17]. In regions with significant temperature differentials, anti-cracking objectives should shift from fatigue resistance to thermal contraction resistance by implementing stress-absorbing layers and strict load limits, thereby establishing a multi-tiered prevention system to significantly extend pavement service life [18].

Funding

Graduate Research and Innovation Project of Chongqing Jiaotong University (Project No.: CYS25493)

Disclosure statement

The authors declare no conflict of interest.

References

[1] Zheng J, Zhou Z, Zhang Q, 2002, Theory and Method of Anti-Cracking Design for Asphalt Pavements. China Communications Press, Beijing.

[2] Sousa J, Shahin M, Harvey J, et al., 2002, Reflective Cracking: The State of the Art. Proceedings of the 9th International Conference on Asphalt Pavements, ISAP, Copenhagen.

[3] Paris P, Erdogan F, 1963, A Critical Analysis of Crack Propagation Laws. Journal of Basic Engineering, 85(4): 528–

534.

[4] Liu J, Zhao Y, Chen S, et al., 2024, Multi-Field Coupling Effects on the Fracture Evolution of Semi-Rigid Base Pavement: A 3D Finite Element Study. Construction and Building Materials, 412: 134145.

[5] Zhao R, Wang L, Chen X, et al., 2025, Evaluation of Steel Slag as Composite Aggregate for Enhancing Anti-Cracking Performance of Asphalt Mixtures. Journal of Cleaner Production, 468: 142156.

[6] Zhang H, Chen X, 2024, Sensitivity Analysis of Asphalt Overlay Service Life Based on Machine Learning and Fracture Mechanics. Materials and Structures, 57(3): 88.

[7] Rice J, 1968, A Path Independent Integral and the Approximate Analysis of Strain Concentration by Notches and Cracks. Journal of Applied Mechanics, 35: 379–386.

[8] Tada H, Paris P, Irwin G, 2000, The Stress Analysis of Cracks Handbook. ASME Press, New York.

[9] Dassault Systèmes, 2022, ABAQUS Theory Manual, Version 2022. Dassault Systèmes, Providence.

[10] Huang Y, 2004, Pavement Analysis and Design. Pearson Education, Upper Saddle River.

[11] Wu K, Zhang Q, 2000, Finite Element Analysis of Reflective Cracking in Asphalt Overlays on Old Cement Concrete Pavements. China Journal of Highway and Transport, 13(2): 7–12.

[12] Kim Y, 2009, Modeling of Asphalt Concrete. McGraw-Hill Education, New York.

[13] Elseifi M, Al-Qadi I, Flints G, et al., 2003, Finite Element Modeling of Overlays Over Cracked Joints in Concrete Pavements. Transportation Research Record, 1852(1): 162–171.

[14] Zhou F, Scullion T, 2005, Overlay Tester: A Simple System to Evaluate the Cracking Resistance of HMA Mixes. Texas Department of Transportation, Austin.

[15] Lytton R, 1989, Use of Geomembranes in Sealing Cracks and Helping to Prevent Reflective Cracking of Asphalt Overlays. Texas Transportation Institute, College Station.

[16] Wang L, Zhang Y, 2025, Mechanistic Analysis of Reflective Cracking in Composite Aggregate Asphalt Overlays Using Advanced Finite Element Modeling. International Journal of Pavement Engineering, 26(1): 112–128.

[17] Li X, Wang H, Zhao J, et al., 2023, Laboratory Evaluation of High-Temperature Performance and Moisture Stability of Steel Slag Asphalt Mixtures. Journal of Materials in Civil Engineering, 35(5): 04023078.

[18] Ministry of Transport of the People's Republic of China, 2017, Specifications for Design of Highway Asphalt Pavements: JTG D50-2017. China Communications Press Co., Ltd., Beijing.